Fossil-Dominated SOA Formation in Coastal China: Size-Divergent Pathways of Aqueous Fenton Reactions versus Gas-phase VOC Autoxidation

Jia-Yuan Wang, Meng-Xue Tang, Shan Lu, Ke-Jin Tang, Xing Peng, Ling-Yan He, Xiao-Feng Huang

Key Laboratory for Urban Habitat Environmental Science and Technology, Peking University Shenzhen Graduate School, Shenzhen, 518055, China.

Corresponding author: Meng-Xue Tang (tangmx@pku.edu.cn)

Abstract: Elucidating size-dependent formation mechanisms of secondary organic aerosols (SOA) remains a critical research gap in atmospheric chemistry. Here, we analyzed water-soluble compounds in size-segregated aerosol samples (0.056–18 μm) collected at a coastal site in southern China. Radiocarbon (^{14}C) isotope analysis reveals that fossil sources dominate SOA in both fine (95.8%) and coarse (80.4%) modes, while the small amount of biogenic SOA mostly existed in the coarse mode (74.1%). Fine-mode oxygenated organic carbon (OOC) correlates strongly with polar carbonyl compounds (e.g., glyoxal, methylglyoxal, acetone, and MVK+MACR), while coarse-mode OOC exhibits better correlations with nonpolar aromatic hydrocarbons (e.g., toluene, C8 aromatic, C9 aromatic, styrene) and biogenic volatile organic compounds (VOCs) (e.g., monoterpenes, isoprene), indicating that the sources of fine- and coarse-mode OOC are different. Multivariate analyses incorporating inorganic ions, pH, water-soluble iron ions, aerosol liquid water content, and O_3 revealed divergent size-dependent mechanisms, emphasizing the significant role of aqueous-phase reactions in fine-mode OOC formation, particularly the key contribution of water-soluble Fe ions ($r^2 = 0.74$), while coarse-mode OOC exhibited a notable correlation with O_3 ($r^2 = 0.63$). Combining the information on VOCs precursors and key components, our study elucidates that aqueous-phase reactions play a key role in fine-mode OOC, especially the Fenton reaction, while gas-phase VOC autoxidation plays an important role in the coarse-mode OOC generation. By examining OOC formation across a wide range of particle sizes, our study highlights the critical need for mode-specific treatment of SOA generation in atmospheric chemical transport modeling.

Key words: Secondary organic aerosol (SOA), Fine mode, Coarse mode, Aqueous-phase reactions, Gas-phase autoxidation

Graphical abstract:

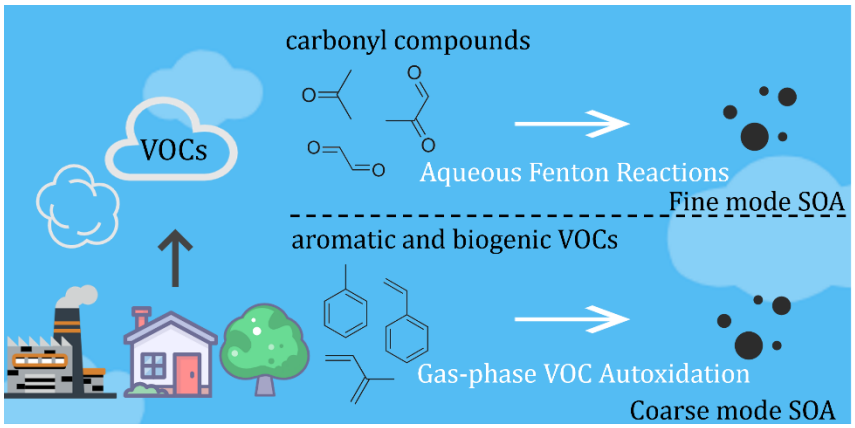

1.Introduction

In urban areas, organic aerosol (OA) constitutes 30–70% of submicron particle mass(Zhang et al., 2017b) , significantly impacting human health, radiation balance, and air quality. OA can originate from direct emissions (primary organic aerosol, POA) or be formed in the atmosphere through the oxidation of semi-volatile and volatile organic compounds (VOCs), resulting in secondary organic aerosol (SOA)(Peng et al., 2021). Globally, SOA is estimated to contribute up to 93% of the total OA budget (Hallquist et al., 2009). However, our understanding of the SOA formation mechanisms is still limited, the complexities of SOA formation are not only due to the presence of large amounts of biogenic and anthropogenic VOC precursors, but also because each VOC can undergo a number of atmospheric degradation processes (e.g., gas-phase radical-mediated oxidation, heterogeneous oxidation, and oligomerization) to produce various condensable oxidized organics (COO) with distinct functionality, reactivity, and volatility(Gu et al., 2023; Xu et al., 2017; Yu et al., 2016).

SOA can be formed from the atmospheric oxidation of VOCs or originate from various processes such as heterogeneous reactions, photochemistry, and aqueous-phase oxidation (Dominutti et al., 2022). Field studies on SOA formation have mostly focused on fine particles (PM_1), partly due to instrument limitations(Xu et al., 2017; Yao et al., 2022a). Recent mass spectrometry-based studies have suggested that photochemical oxidation is a major pathway for SOA formation, typically initiated by reactions with radicals (e.g., OH, NO_3) or oxidants (e.g., O_3), producing a variety of condensable oxidized organics that subsequently engage in gas-to-particle conversion(Xu et al., 2017; Zhan et al., 2021). However, aqueous-phase SOA formation is also an important pathway, with SOA forming on wet aerosols, clouds, and fogs through further chemical processes involving water-soluble organic compounds or the organic products of gas-phase photochemistry(Ervens et al., 2011; Gu et al., 2023; Mei et al., 2025).

While the formation of SOA on coarse particles was mostly neglected, coarse particles (both natural and anthropogenic emissions) are constantly present in the atmosphere and constitute one of the largest contributors to aerosol mass in the troposphere(Wu et al., 2024; Xu et al., 2024), exerting a significant impact on global climate by modulating radiative balance. Coarse particles mainly consist of aluminosilicate, SiO_2, $CaCO_3$, sea salt, and are often coated with secondary organic and inorganic aerosol components under ambient conditions(Li and Shao, 2009; Yang et al., 2024), coarse particles act as reactants or catalysts, enhancing atmospheric heterogeneous reactions and photochemical processes(Pan et al., 2023; Wang et al., 2020b). Heterogeneous and photochemical reactions on mineral dust may play an important role in the formation of coarse-mode SOA (George et al., 2015; He et al., 2022a; Wang et al., 2020b). This also suggests that distinct formation mechanisms may govern fine-mode and coarse-mode secondary organic aerosols.

In this study, we collected a broad range of size-segregated samples (0.056–18 μm) from Shenzhen, a coastal city in southern China, to obtain comprehensive particle size information. We utilized the offline ACSM-PMF method to characterize SOA in these samples and combined it with ^{14}C analysis to gain a deeper understanding of SOA from fossil fuel and biogenic sources (He et al., 2022a; Huang et al., 2020). This study explores the mechanisms of SOA formation across both fine-mode and coarse-mode, enhancing our understanding of the diverse generation mechanisms of SOA across various particle size distributions.

2.Material and methods

2.1 Sampling site and sample collection

The sampling site, Atmospheric Observation Supersite of Shenzhen (AOSS, 22.60 °N, 113.98 °E), is

77 located at an urban site in the southeast of the Pearl River Delta (PRD) region. There are no significant
78 local pollution sources in the vicinity. The sampling period encompassed both the peak of particulate
79 matter pollution and the most severe photochemical pollution in Shenzhen for the year. The levels of
80 VOCs at this site are typically influenced by continental air masses, marine air masses, and local biogenic
81 emissions(Li et al., 2024a). A ten-stage micro-orifice uniform deposit impactor (MOUDI, model 110,
82 MSP Co., USA) with aerodynamic diameter cut-points of 0.056, 0.1, 0.18, 0.32, 0.56, 1.0, 1.8, 3.2, 5.6,
83 10, and 18 μm was used to collect size-segregated aerosol samples on Teflon filters from 21 October
84 2022 to 3 February 2023.In this study, we found that 1–1.8 μm particles showed more coarse mode
85 properties, so we took 1 μm as the division boundary, so we use 1 μm as the as the boundary between
86 fine particles and coarse particles, in this study. The sampling flow rate was 30 L/min. The average
87 ambient temperature during the sampling period was 20.0 °C, and the dominant wind direction was
88 northeasterly. In total, one hundred and sixty samples were collected with a sampling cycle of 72 hours.

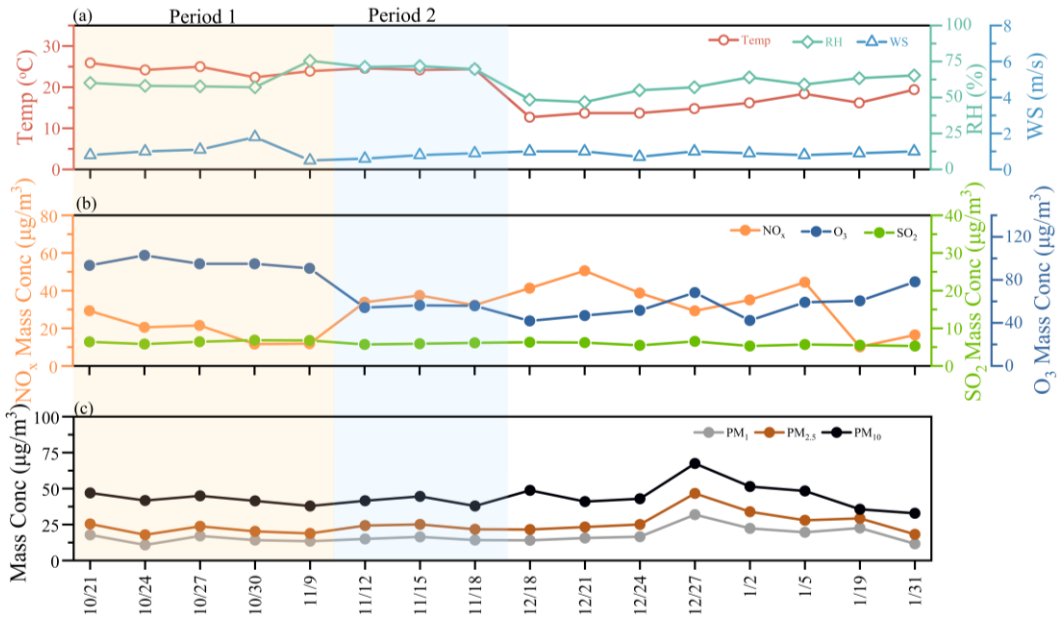

89

90 **Figure 1.** Time series of relative humidity (RH), Temperature (Temp) and wind speed (WS) (a), O_3,
91 $SO_2$and NO_x (b), PM_1, $PM_{2.5}$ and PM_{10}(c). The time series were categorized to be two typical periods
92 based on total O_3 mass concentrations: the high-O_3 period (Period 1), and the low-O_3 period (Period 2).

2.2. Chemical analysis

The mass of the size-segregated aerosol samples was obtained from the difference in mass of the Teflon filter before and after sampling in a cleanroom at conditions of 22.1 ℃ and 49.2% relative humidity. Then, each filter was extracted with 20 mL of ultrapure water in an ultrasonic bath with ice for 30 min and then filtered with a 0.22 μm Teflon filter for further analysis. A portion of the water extract was analyzed for water-soluble metal elements using an inductively coupled plasma mass spectrometer (ICP-MS, Bruker auroraM90, Germany). Inorganic ions (Cl^-, SO_4^{2-} , NO_3^- , NH_4^+, Na^+, K^+, Mg^{2+}, Ca^{2+}) were measured using an ion chromatography system (ICS-6000, Dionex, USA). A portion was analyzed for water-soluble organic matter (WSOM) and the corresponding mass spectra using a Nebulizer-ACSM system (ToF-ACSM-X, Aerodyne Research, Inc., USA) and a portion was analyzed for water-soluble organic carbon (WSOC) with a total organic carbon analyzer (N/C 3100, Analytik Jena AG, Germany) to quantify water-soluble organic oxygen (WSOO), the major ion fragments (m/z 44, m/z 56,m/z 57, m/z 58) and elements(C, H, O, and N) measured by ToF-ACSM-X. Equal amounts of the water extract from the same MOUDI stages were combined and concentrated for ^{14}C analysis based on accelerator mass spectrometry. More details of the Nebulizer-ACSM and radiocarbon can be found in(He et al., 2022a; Huang et al., 2020).

2.3 Other measurements

A meteorological monitoring instrument (WXT536, Vaisala, Finland) was used to measure the meteorological variables, including atmospheric temperature (Temp), relative humidity (RH), wind direction (WD), and wind speed (WS). Criteria air pollutants were monitored using the following instruments: a 5030i $PM_{2.5}$ and 5030i PM_{10} for particulate matter, a 43i SO_2 analyzer, a 42i NO_x analyzer, a 49i O_3 analyzer, and a 48i CO analyzer (Thermo Scientific, USA). Additionally, PTR-ToF-MS (6000X2,

Ionicon Analytik GmbH, Austria) with H_3O^+ ionization mode was used for online measurements of volatile organic compounds at the same site during the campaign. Further details regarding the PTR-ToF-MS are available in (He et al., 2022b; Li et al., 2024b).

2.4 Data analysis

The inorganic ion components of size-segregated aerosol samples (Cl^-, SO_4^{2-} , NO_3^- , Na^+,NH_4^+, K^+, Mg^{2+}, Ca^{2+}), along with relative humidity (RH) and temperature were input into ISORROPIA II model to calculate the aerosol liquid water content (ALWC) and aerosol pH ($pH_{aerosol}$), the thermodynamic equilibrium model ISORROPIA II was used to estimate the size-resolved ALWC and $pH_{aerosol}$ in this study owing to its accuracy, reliability, and high computational efficiency(Duan et al., 2020; Tan et al., 2017; Xu et al., 2024). The Pearson correlation method was applied using SPSS Statistics software for correlation analysis. Quantitative source apportionment of water-soluble organic carbon (WSOC) was conducted with the U.S. EPA PMF v5.0 software. Data matrices and error matrix of WSOC, WSOO, CO_2^+, $C_4H_9^+$, and nss-K^+ for a total of 160 samples (16 sets × 10 stages) were input into the PMF model, the three-factor (the more oxidized oxygenated organic carbon (MO-OOC), the less oxidized OOC (LO-OOC), and biomass-burning organic carbon (BBOC) determined to be the most reasonable solution (Figure S1).More details of the source apportionment of WSOC by PMF modeling are provided in the supporting information. Considering the significant contribution of sea salt at the sampling site, non-sea-salt potassium (nss-K^+) was calculated to better represent biomass burning emissions. Nss-K^+ was calculated from measured K^+ assuming the mass ratio K^+/Na^+ of 0.036 as in seawater, following the approach in (Boreddy and Kawamura, 2015; Klopper et al., 2020).

3 Results and discussion

3.1 average size distributions of the aerosol components

Figure 2a shows the average size distributions of the aerosol components, coarse modes exhibit higher mass concentrations, accounting for 66.7% of the total mass. The coarse mode contains significantly higher proportions of water-insoluble components, with measured concentrations reaching 20.63 μg/m^3, accounting for 75.6% of the total coarse-mode mass concentration. Unlike the coarse mode, the fine mode has a higher proportion of water-soluble components. As is shown in Figure 2b, the main water-soluble inorganic ions in the fine mode differ from those in the coarse mode, sulfate (SO_4^{2-}) and ammonium (NH_4^+) are the most abundant compounds in the fine mode, constituting 17.0% and 7.4% of the total mass of fine particles, respectively. In contrast, nitrate (NO_3^-) and calcium (Ca^{2+}) are the predominant inorganic ions in the coarse mode, comprising 5.6% and 1.5% of the total mass of coarse particles, respectively. Although the compositions of fine- and coarse-mode water-soluble inorganic ions differ significantly, WSOM is the most abundant water-soluble component in both modes. WSOM constitutes 55.9% of the total water-soluble mass in fine particles and 40.9% in coarse particles, underscoring its critical role in both size modes.

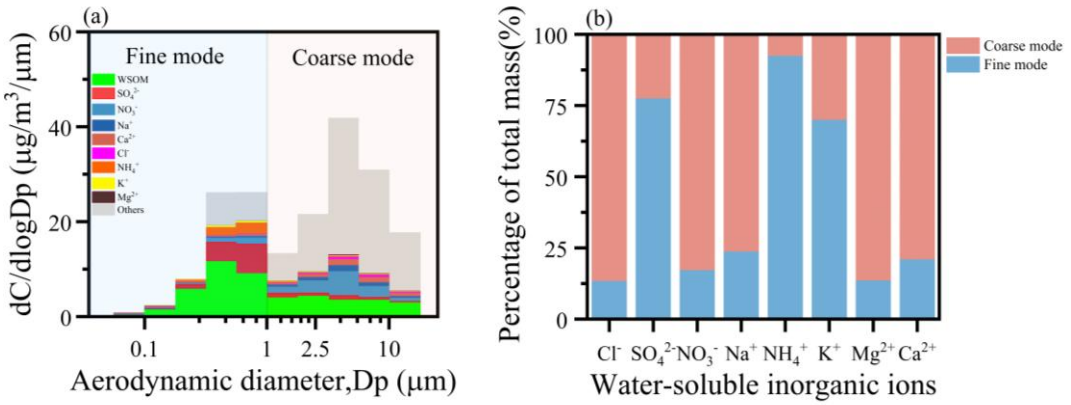

151

152 **Figure 2.** The average size distributions of aerosol components at this site (a), the percentage of the fine
153 mode and coarse mode of water-soluble inorganic ions (b). The "others" category was calculated by the
154 mass concentration of particulate matter minus the total concentrations of water-soluble species, and
155 might include non-water soluble organic matter, elemental carbon, crustal material, etc.

156 **3.2 Possible sources of fine and coarse mode SOA**

157 In this study, PMF is used to extract OA components. The three-factor solution was considered the most
158 reasonable based on the clarity of factor profiles and the residual distribution. Further details are provided
159 in the Supplement. Figure 3a presents the contributions of oxygenated organic carbon (OOC), defined as
160 the sum of MO-OOC (moderately oxygenated organic carbon) and LO-OOC (lowly oxygenated organic
161 carbon), as well as Biomass Burning Organic Carbon (BBOC), across all particle size bins. The results
162 indicate that BBOC was mainly disturbed in the fine mode accounting for 91.1% of the total BBOC.
163 OOC dominated in both the fine (64.4%) and coarse mode (88.4%), and previous studies found that the
164 fine mode SOA can be estimated by WSOC after removing the contribution of biomass burning(He et
165 al., 2022b; Huang et al., 2020), in this study , OOC is equivalent to SOA. This highlights the critical role
166 of SOA in both the fine and coarse mode.

167 Figure 3b shows the size distributions of fossil fuel OOC and biogenic OOC in all size bins, which

were calculated by combining the results from the PMF factor contributions and the ^{14}C isotope analysis, and the calculations were performed as in our previous study with equations (1)-(3) (He et al., 2022a; Huangetal.,2020) :

$$\text{biogenic carbon} = \text{WSOC} * f_{modern} \quad (1)$$

$$\text{biogenic OOC} = \text{biogenic carbon} - \text{BBOC} \quad (2)$$

$$\text{fossil fuel OOC} = \text{OOC} - \text{biogenic OOC} \quad (3)$$

Here, f_{modern} represents the modern carbon fraction, defined as the ratio of the $^{14}C/^{12}C$ content in a sample relative to that of a modern standard (NBS Oxalic Acid I from AD 1950), corrected for $\delta^{13}C$ isotopic fractionation and ^{14}C decay(Zhang et al., 2019). Biogenic carbon represents the portion of carbon derived from biogenic sources, biogenic OOC represents the oxygenated organic carbon originating from biogenic sources, fossil fuel OOC represents the oxygenated organic carbon derived from fossil fuel sources.

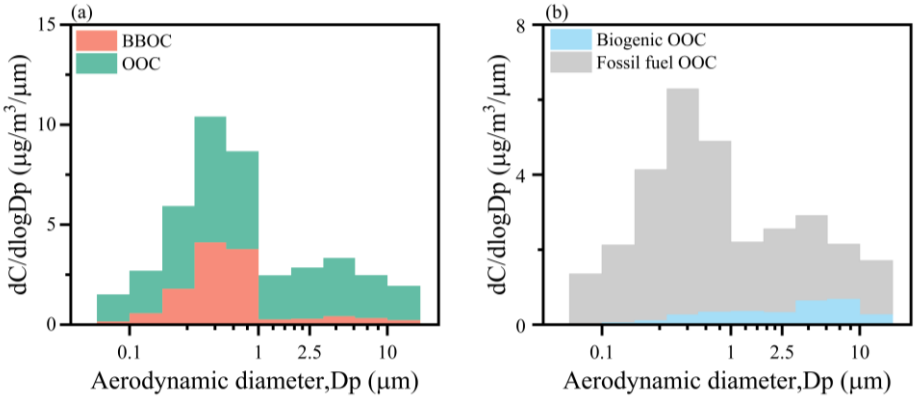

Figure 3. Average size distributions of the WSOC compositions, OOC and BBOC (a), fossil fuel OOC and biogenic OOC(b).

After removing the contributions from BBOC, the results clearly indicate that fossil fuel organic carbon (OOC) dominates in both fine (95.8%) and coarse (80.4%) modes, reflecting the significant role

of anthropogenic sources in SOA generation. Regarding particle size distribution, fossil fuel OOC is predominantly found in the fine mode (66.0%), while biogenic OOC is mainly present in the coarse mode (74.1%). This distribution indicates the differing reaction pathways for SOA in fine and coarse modes.

We further explore the relationship between fine- and coarse-mode OOC and gaseous precursors, more details of the gaseous precursors are provided in the supporting information (Table S2). We observed a high correlation between fine-mode OOC and polar carbonyl compounds, such as glyoxal, methylglyoxal, acetone, and MVK+MACR (Table 1). Carbonyl compounds are first- and/or second-generation gas-phase oxidation products of both anthropogenic (e.g., aromatics, acetylene) and biogenic (e.g., isoprene) sources (Ervens et al., 2011), this also suggests a complex source profile for fine mode SOA. Additionally, carbonyl compounds have strong water solubility and can be absorbed into clouds and fog to react with ·OH to form oligomers, which promote the formation of SOA(Wang et al., 2022).In contrast, coarse-mode OOC exhibited significant negative correlations with nonpolar aromatic hydrocarbons (e.g., toluene, C8 aromatic, C9 aromatic, styrene) and biogenic VOCs (monoterpenes) (Table 1). Despite these negative correlations, several evidence support atmospheric relevance of these gaseous precursors to coarse-mode SOA. Firstly, the correlations with aromatic and biogenic VOCs were unique to coarse-mode OOC and not observed in the fine-mode OOC, clearly demonstrating distinct precursor pathways for coarse and fine-mode SOA. Secondly, ^{14}C isotope analysis explicitly confirmed that coarse-mode OOC consisted of both fossil (approximately 80.4%) and biogenic (approximately 19.6%) components, directly aligning with the respective aromatic and biogenic VOC precursors identified here. Thirdly, biogenic OOC was found predominantly in coarse-mode particles (74.1%), providing direct observational evidence linking biogenic VOC oxidation products to coarse-mode aerosol formation. This revealed different gaseous precursors for fine- and coarse-mode SOA, and reflected the different SOA

207 generation mechanisms that may exist.

208 **Table 1.** The correlation coefficients between OOC and typical VOCs in the campaign. * indicates a
209 significance level of 95% ($p < 0.05$).

	Monoterpenes	Isoprene	MVK+MACR	Toluene	C8 aromatic	C9 aromatic	Styrene	Glyoxal	Methylglyoxal	Acetone
Fine mode OOC	0.20	0.47	0.70*	0.38	0.39	0.36	0.46	0.70*	0.73*	0.62*
Coarse mode OOC	-0.75*	-0.56	-0.34	-0.60*	-0.65*	-0.66*	-0.74*	-0.39	-0.39	-0.52

210 **3.3 Possible formation mechanisms for fine mode SOA**

211 The previous results reveal a distinct origin for fine and coarse mode OOC, suggesting different SOA
212 generation mechanisms. Therefore, additional field measurements are necessary to further understand
213 the mechanisms and key factors affecting SOA formation.

214 Building on the findings from the previous section that fine-mode OOC are primarily derived from
215 carbonyl compounds, it is noteworthy that carbonyl compounds are highly reactive and exhibit
216 significant water solubility(Liu et al., 2022; Wang et al., 2022; Xu et al., 2022). These properties enable
217 them to contribute significantly to SOA formation through aqueous-phase reactions, particularly for
218 dicarbonyls such as glyoxal (Gly, CHOCHO) and methylglyoxal (Mgly, CH_3COCHO), which have been
219 identified as key SOA precursors (Liu et al., 2022; Tan et al., 2017) . Previous studies have identified
220 characteristic fragment ions of glyoxal and methylglyoxal (e.g., $C_2O_2^+$ and $CH_2O_2^+$), detected by aerosol
221 mass spectrometer (AMS) and aerosol chemical speciation monitor (ACSM), which play a crucial role
222 in the formation of low-volatility SOA during cloud processing and are strongly correlated with aqueous
223 oxygenated organic aerosol (aq-OOA) (Duan et al., 2020; Sun et al., 2016). As shown in Figure 4a, these
224 fragment ions are predominantly distributed in fine particles, indicating the significance of aqueous-
225 phase processing in the fine mode. Further evidence of aqueous-phase reactions is provided by the
226 behavior of MVK and MACR. While the direct aqueous-phase reaction of MVK and MACR with ozone

is less competitive compared to the faster OH-initiated reactions (Chen et al., 2008) , aerosol liquid water content (ALWC) serves as a key metric for characterizing aqueous-phase SOA formation due to its positive correlation with these processes, especially under conditions of high relative humidity and elevated NO_x levels (Kuang et al., 2020b; McNeill, 2015; Zhan et al., 2021). In this study, we observed a strong positive correlation between fine-mode OOC and ALWC (Figure 4b), suggesting that fine-mode SOA is predominantly generated through aqueous-phase processes.

However, in contrast to the coarse mode, in contrast to the coarse modes, the fine modes are not abundant in ALWC (Figure S6). Despite this, we observed a significant relationship between OOC and ALWC exclusively in the fine mode. To further investigate the behavior of carbonyl compounds under the unique conditions of the fine mode, we analyzed the correlations of fine- and coarse-mode OOC with key factors, revealing notable differences between the two modes. First, the fine mode is characterized by higher concentrations of inorganic ions, such as sulfate and nitrate, which may play a critical role in SOA formation. Specifically, sulfate demonstrated a stronger positive influence on fine-mode OOC formation compared to nitrate, as evidenced by their respective correlation coefficients (R^2 = 0.85 for sulfate, Figure 4c; R^2 = 0.47 for nitrate, Figure 4d). This discrepancy may arise from the fact that sulfate (SO_4^{2-}) is primarily produced through aqueous-phase reactions, whereas nitrate (NO_3^-) is predominantly generated via gas-phase reactions (Zhan et al., 2021) . Additionally, the fine mode exhibits acidic conditions ($pH_{aerosol}$ = 0.4–4.3), and we observed distinct correlations between fine-mode OOC and $pH_{aerosol}$ (Figure 4e). This suggests that the lower pH in the fine mode favors the formation of fine-mode OOC.

A few studies have emphasized the significant role of metal ions in SOA formation, particularly under low pH conditions. To further investigate this, we examined the correlation between water-soluble metal

ions and fine-mode OOC (Table S5). Our analysis revealed that fine-mode OOC exhibits a strong correlation with water-soluble Fe ions ($r = 0.82$, $p < 0.05$), and a positive relationship was observed between the concentration of iron ions and fine-mode OOC (Figure 5f). Additionally, water-soluble iron ions were found to be highly concentrated in the fine mode (Figure S4), with their concentration (18.87 ng/m^3) significantly exceeding that of other metal ions. Recent studies have highlighted the role of water-soluble Fe ions in Fenton chemistry, where they cycle between Fe^{2+} and Fe^{3+}. This process, particularly through Fenton reactions involving peroxides, may substantially enhance SOA formation by supplying particle-phase oxidants(Qin et al., 2022; Ye et al., 2021). Specifically, Fenton reactions within aqueous particles can generate OH radicals,, which oxidize organic compounds such as carbonyls, especially under lower pH conditions (Kuang et al., 2020a).

Therefore, in this study, we propose that aqueous-phase reactions play a dominant role in the formation of fine-mode SOA. The lower pH and elevated concentrations of water-soluble Fe ions in the fine mode create favorable conditions for SOA formation from carbonyl compounds, primarily through Fenton reactions.

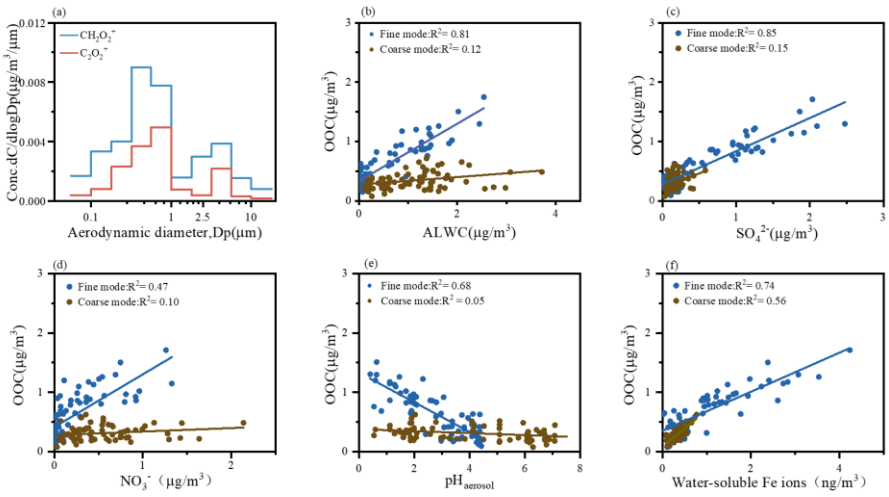

Figure 4. Average size distributions of $CH_2O_2^+$, and $C_2O_2^+$ (a), and relationship between OOC and ALWC (b), SO_4^{2-}(c), NO_3^-(d), $pH_{aerosol}$(e), water-soluble iron ions(f).

3.4 Possible formation mechanisms for coarse mode SOA

Most previous studies have focused on the heterogeneous uptake of inorganic trace gases by coarse particles, while the interaction between VOCs and coarse particles remains largely unexplored. Consequently, the role of coarse particles in SOA formation and growth under typical polluted urban conditions is still poorly understood(Yu et al., 2016; Yu and Jang, 2019).

A distinct phenomenon observed in our experiments is that biogenic-OOC are predominantly distributed in the coarse mode, which may be attributed to unique SOA formation pathways in this mode. Biogenic-OOC is primarily generated through the oxidation of BVOCs by atmospheric oxidants such as OH radicals, O_3, and NO_3radicals, (Gagan et al., 2023). BVOCs emitted by terrestrial vegetation, including isoprene and monoterpenes, significantly contribute to the total SOA budget. As shown in Table 1, coarse-mode OOC exhibits a strong correlation with monoterpenes ($r = -0.75$, $p < 0.05$) but a weaker correlation with isoprene ($r = -0.56$, $p < 0.05$), suggesting that monoterpenes play a more prominent role in biogenic-OOC formation.

Regarding the mechanisms of SOA generation from monoterpenes and isoprene, isoprene primarily reacts with OH radicals to form SOA, whereas monoterpenes, in addition to reacting with OH radicals, also undergo significant SOA formation through reactions with O_3 (McFiggans et al., 2019; Xu et al., 2015). Previous studies have demonstrated that monoterpene-derived SOA is more oxidized in the presence of nitrate-containing seed aerosols compared to ammonium sulfate seed aerosols (Huang et al., 2016; Watne et al., 2017). The higher nitrate concentrations in the coarse mode further favor the O_3 oxidation pathway for monoterpenes. Our sampling site, located in the PRD region, is one of the most rapidly urbanized areas with high anthropogenic emissions (Ma et al., 2024). The sampling period coincided with elevated O_3 pollution levels. Coarse-mode particles, characterized by higher pH compared

to fine-mode particles, create conditions conducive to photosensitive reactions and O_3 oxidation pathways (Yu and Jang, 2019). Further analysis reveals a strong correlation between coarse-mode OOC and O_3 (Figure 5a). Additionally, Figure 5b demonstrates that coarse-mode OOC concentrations are significantly higher during high-O_3 periods compared to low-O_3 periods, with a distinct peak observed during high-O_3 episodes. Notably, no significant increase in the concentrations of other inorganic ions was observed during these high-O_3 periods (Figure S6). These findings collectively underscore the critical role of O_3 in the formation of coarse-mode SOA.

However, the reaction pathways involved in coarse-mode SOA formation remain poorly understood. The ^{14}C isotope analysis results indicate that fossil fuel-derived OOC are the primary source of coarse-mode OOC. Additionally, coarse-mode OOC exhibits a stronger correlation with aromatic VOCs, particularly styrene (Table 1). However, since nonpolar aromatic hydrocarbons do not directly react with O_3 to form SOA, further investigation is needed to elucidate the role of O_3 in coarse-mode SOA formation. Recent studies have highlighted the rapid gas-phase autoxidation of endocyclic alkenes initiated by ozonolysis, which yields highly oxygenated organic molecules (HOMs), particularly from monoterpenes and aromatic compounds (Rissanen, 2021). Chemistry transport models have demonstrated that ozonolysis of monoterpenes accounts for 79% of HOMs production (Shi et al., 2021). Additionally, photochemical oxidation of substituted aromatic compounds has been shown to form HOMs through rapid intramolecular autoxidation reactions, a process analogous to the oxidation of monoterpenes. O_3 can facilitate these reactions during the photo-oxidation of aromatics (Molteni et al., 2018; Suh et al., 2003; Wang et al., 2020a) , which partially explains the stronger correlation between O_3 and coarse-mode OOC. This conclusion is further supported by the higher oxidation state (O/C ratio) observed in the coarse mode compared to the fine mode (Figure 5c).

Moreover, recent studies have identified carboxylic acids as products of these reactions (Zhang et al., 2017a). The slope of coarse-mode OOC in the Van Krevelen (VK) plot is close to -0.5 (Figure 5d), indicating the large formation of carboxylic acids with fragmentation through the replacement of hydrogen atoms. The coarse mode is characterized by higher ALWC, higher pH, and favorable partitioning of reaction products into the particulate phase. Based on these findings, we propose that gas-phase autoxidation plays a significant role in the formation of coarse-mode SOA.

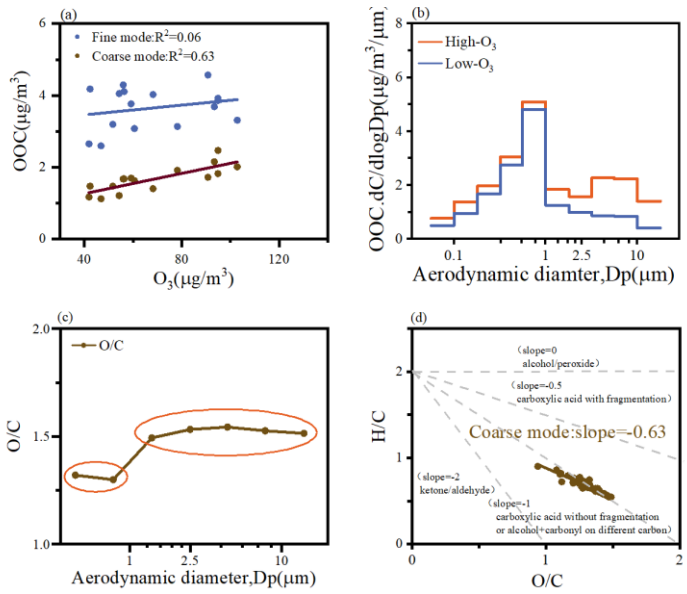

Figure 5. Relationship between OOC and O_3 (a), average size distributions of OOC (b), and organic O/C(c), Van Krevelen diagram of H / C vs. O / C(d).

4 Summary and implications

This study collected 16 sets of size-segregated aerosol samples (0.056–18 μm) in Shenzhen, a coastal city in the Pearl River Delta, from October 2022 to January 2023. The water-soluble components, including typical inorganic ions, water-soluble organic compounds, and water-soluble metal ions, were analyzed, and WSOM emerged as the most abundant water-soluble component in both modes, accounting for 55.9% and 40.9% of the total water-soluble mass in fine and coarse particles, respectively. This

highlights the critical role of WSOM in both size fractions.

Our findings indicate that WSOM in both fine and coarse modes exhibits secondary production. To quantify SOA by using OOC as a surrogate measure, we applied PMF modeling and utilized radiocarbon isotopes to distinguish between fossil fuel-derived and biogenic OOC. Radiocarbon (^{14}C) isotope analysis reveals that fossil sources dominate SOA in both fine (95.8%) and coarse (80.4%) modes, while the small amount of biogenic SOA mostly existed in the coarse mode (74.1%), we emphasize the significant contribution of anthropogenic VOCs to SOA formation in coastal atmospheres, where high relative humidity and enhanced atmospheric oxidation capacity also play pivotal roles in SOA generation across both fine and coarse modes. Furthermore, we investigated potential precursor sources for fine- and coarse-mode OOC, fine-mode OOC correlates strongly with polar carbonyl compounds (e.g., glyoxal, methylglyoxal, acetone, and MVK+MACR), while coarse-mode OOC exhibits better correlations with nonpolar aromatic hydrocarbons (e.g., toluene, C8 aromatic, C9 aromatic, styrene) and biogenic VOCs (e.g., monoterpenes, isoprene), indicating that the sources of fine- and coarse-mode OOC are different, indicating that the sources of fine- and coarse-mode OOC are different, indicating distinct precursor sources for SOA in different size modes.

Multivariate analyses incorporating inorganic ions, pH, water-soluble Fe ions, aerosol liquid water content, and O_3 revealed divergent size-dependent mechanisms, emphasizing the significant role of aqueous-phase reactions in fine-mode OOC formation, particularly the key contribution of water-soluble iron ions (r^2 = 0.74), while coarse-mode OOC exhibited a notable correlation with O_3 (r^2 = 0.63). Combining the information on VOCs precursors and key components, our study elucidates that aqueous-phase reactions play a key role in fine-mode OOC, especially the Fenton reaction, while gas-phase autoxidation plays an important role in the coarse-mode OOC generation. By examining OOC formation

across a wide range of particle sizes, this study provides novel insights into SOA formation mechanisms and enhances our understanding of the formation pathways of SOA in both fine and coarse mode.

However, the specific mechanisms governing SOA generation in different particle size ranges remain poorly understood. We strongly recommend further laboratory experiments to explore these mechanisms in greater depth. Notably, our study underscores the significant role of anthropogenic VOCs in SOA formation in coastal environments, where high relative humidity and atmospheric oxidation capacity are critical drivers. Similar conditions are prevalent in marginal seas and estuaries near urban areas, warranting further in-depth studies in these representative regions.

Data availability. Datasets are available by contacting the corresponding author, Meng-Xue Tang (tangmx@pku.edu.cn)

Supplement. The supplement material related to this article is available online at:

Author contributions. J.-Y.W., M.-X.T., and X.-F.H. conceptualized the study. J.-Y.W., S.L., and K.-J.T executed the experiments. J.-Y.W., M.-X.T., and X.P. carried out the statistical analysis. J.-Y.W. prepared the first draft of the manuscript, which was commented on and revised by M.-X.T., L.-Y.H., and X.-F.H. All authors reviewed and approved the final version for publication.

Competing interests. The authors declare that they have no conflict of interest.

Financial support. This work was supported by the National Key Research and Development Program of China (2022YFC3701000, Task2) and the National Natural Science Foundation of China (42407145).

Reference

Boreddy, S. K. R. and Kawamura, K.: A 12-year observation of water-soluble ions in TSP aerosols collected at a remote marine location in the western North Pacific: an outflow region of Asian dust, Atmospheric Chem. Phys., 15, 6437–6453, 2015.

Chen, Z. M., Wang, H. L., Zhu, L. H., Wang, C. X., Jie, C. Y., and Hua, W.: Aqueous-phase ozonolysis of methacrolein and methyl vinyl ketone: a potentially important source of atmospheric aqueous oxidants, Atmos Chem Phys, 2008.

Dominutti, P. A., Chevassus, E., Baray, J.-L., Jaffrezo, J.-L., Borbon, A., Colomb, A., Deguillaume, L., El Gdachi, S., Houdier, S., Leriche, M., Metzger, J.-M., Rocco, M., Tulet, P., Sellegri, K., and Freney, E.: Evaluation of the Sources, Precursors, and Processing of Aerosols at a High-Altitude Tropical Site, ACS Earth Space Chem., 6, 2412–2431, 2022.

Duan, J., Huang, R.-J., Li, Y., Chen, Q., Zheng, Y., Chen, Y., Lin, C., Ni, H., Wang, M., Ovadnevaite, J., Ceburnis, D., Chen, C., Worsnop, D. R., Hoffmann, T., O'Dowd, C., and Cao, J.: Summertime and wintertime atmospheric processes of secondary aerosol in Beijing, Atmospheric Chem. Phys., 20, 3793–3807, 2020.

Ervens, B., Turpin, B. J., and Weber, R. J.: Secondary organic aerosol formation in cloud droplets and aqueous particles (aqSOA): a review of laboratory, field and model studies, Atmospheric Chem. Phys., 11, 11069–11102, 2011.

Gagan, S., Sarang, K., Rudzinski, K. J., Liu, R., Szmigielski, R., and Zhang, Y.: Synthetic strategies for oxidation products from biogenic volatile organic compounds in the atmosphere: A review, Atmos. Environ., 312, 120017, 2023.

George, C., Ammann, M., D'Anna, B., Donaldson, D. J., and Nizkorodov, S. A.: Heterogeneous Photochemistry in the Atmosphere, Chem. Rev., 115, 4218–4258, 2015.

Gu, Y., Huang, R.-J., Duan, J., Xu, W., Lin, C., Zhong, H., Wang, Y., Ni, H., Liu, Q., Xu, R., Wang, L., and Li, Y. J.: Multiple pathways for the formation of secondary organic aerosol in the North China Plain in summer, Atmospheric Chem. Phys., 23, 5419–5433, 2023.

Hallquist, M., Wenger, J. C., Baltensperger, U., Rudich, Y., Simpson, D., Claeys, M., Dommen, J., Donahue, N. M., George, C., Goldstein, A. H., Hamilton, J. F., Herrmann, H., Hoffmann, T., Iinuma, Y., Jang, M., Jenkin, M. E., Jimenez, J. L., Kiendler-Scharr, A., Maenhaut, W., McFiggans, G., Mentel, T. F., Monod, A., Prévôt, A. S. H., Seinfeld, J. H., Surratt, J. D., Szmigielski, R., and Wildt, J.: The formation, properties and impact of secondary organic aerosol: current and emerging issues, Atmospheric Chem. Phys., 9, 5155–5236, 2009.

He, D.-Y., Huang, X.-F., Wei, J., Wei, F.-H., Zhu, B., Cao, L.-M., and He, L.-Y.: Soil dust as a potential bridge from biogenic volatile organic compounds to secondary organic aerosol in a rural environment, Environ. Pollut., 298, 118840, 2022a.

He, D.-Y., Huang, X.-F., Wei, J., Wei, F.-H., Zhu, B., Cao, L.-M., and He, L.-Y.: Soil dust as a potential bridge from biogenic volatile organic compounds to secondary organic aerosol in a rural environment, Environ. Pollut., 298, 118840, 2022b.

Huang, D. D., Zhang, X., Dalleska, N. F., Lignell, H., Coggon, M. M., Chan, C., Flagan, R. C., Seinfeld, J. H., and Chan, C. K.: A note on the effects of inorganic seed aerosol on the oxidation state of secondary organic aerosol— α -Pinene ozonolysis, J. Geophys. Res. Atmospheres, 121, 2016.

Huang, X.-F., Dai, J., Zhu, Q., Yu, K., and Du, K.: Abundant Biogenic Oxygenated Organic Aerosol in Atmospheric Coarse Particles: Plausible Sources and Atmospheric Implications, Environ. Sci. Technol., 54, 1425–1430, 2020.

Jimenez, J. L., Canagaratna, M. R., Donahue, N. M., Prevot, A. S. H., Zhang, Q., Kroll, J. H., DeCarlo,

412 P. F., Allan, J. D., Coe, H., Ng, N. L., Aiken, A. C., Docherty, K. S., Ulbrich, I. M., Grieshop, A. P.,
413 Robinson, A. L., Duplissy, J., Smith, J. D., Wilson, K. R., Lanz, V. A., Hueglin, C., Sun, Y. L., Tian,
414 J., Laaksonen, A., Raatikainen, T., Rautiainen, J., Vaattovaara, P., Ehn, M., Kulmala, M., Tomlinson,
415 J. M., Collins, D. R., Cubison, M. J., E., Dunlea, J., Huffman, J. A., Onasch, T. B., Alfarra, M. R.,
416 Williams, P. I., Bower, K., Kondo, Y., Schneider, J., Drewnick, F., Borrmann, S., Weimer, S.,
417 Demerjian, K., Salcedo, D., Cottrell, L., Griffin, R., Takami, A., Miyoshi, T., Hatakeyama, S.,
418 Shimono, A., Sun, J. Y., Zhang, Y. M., Dzepina, K., Kimmel, J. R., Sueper, D., Jayne, J. T., Herndon,
419 S. C., Trimborn, A. M., Williams, L. R., Wood, E. C., Middlebrook, A. M., Kolb, C. E., Baltensperger,
420 U., and Worsnop, D. R.: Evolution of Organic Aerosols in the Atmosphere, Science, 326, 1525–1529,
421 https://doi.org/10.1126/science.1180353, 2009.
422 Klopper, D., Formenti, P., Namwoonde, A., Cazaunau, M., Chevaillier, S., Feron, A., Gaimoz, C., Hease,
423 P., Lahmidi, F., Mirande-Bret, C., Triquet, S., Zeng, Z., and Piketh, S. J.: Chemical composition and
424 source apportionment of atmospheric aerosols on the Namibian coast, Atmos Chem Phys, 2020.
425 Kuang, X. M., Gonzalez, D. H., Scott, J. A., Vu, K., Hasson, A., Charbouillot, T., Hawkins, L., and
426 Paulson, S. E.: Cloud Water Chemistry Associated with Urban Aerosols: Rapid Hydroxyl Radical
427 Formation, Soluble Metals, Fe(II), Fe(III), and Quinones, ACS Earth Space Chem., 4, 67–76, 2020a.
428 Kuang, Y., He, Y., Xu, W., Yuan, B., Zhang, G., Ma, Z., Wu, C., Wang, C., Wang, S., Zhang, S., Tao, J.,
429 Ma, N., Su, H., Cheng, Y., Shao, M., and Sun, Y.: Photochemical Aqueous-Phase Reactions Induce
430 Rapid Daytime Formation of Oxygenated Organic Aerosol on the North China Plain, Environ. Sci.
431 Technol., 54, 3849–3860, 2020b.
432 Li, W. J. and Shao, L. Y.: Observation of nitrate coatings on atmospheric mineral dust particles, Atmos
433 Chem Phys, 2009.

Li, Z.-J., He, L.-Y., Ma, H.-N., Peng, X., Tang, M.-X., Du, K., and Huang, X.-F.: Sources of atmospheric oxygenated volatile organic compounds in different air masses in Shenzhen, China, Environ. Pollut., 340, 122871, 2024a.

Li, Z.-J., He, L.-Y., Ma, H.-N., Peng, X., Tang, M.-X., Du, K., and Huang, X.-F.: Sources of atmospheric oxygenated volatile organic compounds in different air masses in Shenzhen, China, Environ. Pollut., 340, 122871, 2024b.

Liu, Q., Gao, Y., Huang, W., Ling, Z., Wang, Z., and Wang, X.: Carbonyl compounds in the atmosphere: A review of abundance, source and their contributions to O3 and SOA formation, Atmospheric Res., 274, 106184, 2022.

Ma, F., Wang, H., Ding, Y., Zhang, S., Wu, G., Li, Y., Gong, D., Ristovski, Z., He, C., and Wang, B.: Amplified Secondary Organic Aerosol Formation Induced by Anthropogenic–Biogenic Interactions in Forests Around Megacities, J. Geophys. Res. Atmospheres, 129, e2024JD041679, 2024.

McFiggans, G., Mentel, T. F., Wildt, J., Pullinen, I., Kang, S., Kleist, E., Schmitt, S., Springer, M., Tillmann, R., Wu, C., Zhao, D., Hallquist, M., Faxon, C., Le Breton, M., Hallquist, Å. M., Simpson, D., Bergström, R., Jenkin, M. E., Ehn, M., Thornton, J. A., Alfarra, M. R., Bannan, T. J., Percival, C. J., Priestley, M., Topping, D., and Kiendler-Scharr, A.: Secondary organic aerosol reduced by mixture of atmospheric vapours, Nature, 565, 587–593, 2019.

McNeill, V. F.: Aqueous Organic Chemistry in the Atmosphere: Sources and Chemical Processing of Organic Aerosols, Environ. Sci. Technol., 49, 1237–1244, 2015.

Mei, S., Xia, K., Liu, C., Chen, X., Yuan, R., Liu, H., Zhao, C., and Liu, S.: Aqueous-Phase Processing Affects the Formation and Size Distribution of Aerosol Organic Functional Groups During Heavy Pollution, J. Geophys. Res. Atmospheres, 130, e2024JD042029, 2025.

Molteni, U., Bianchi, F., Klein, F., El Haddad, I., Frege, C., Rossi, M. J., Dommen, J., and Baltensperger, U.: Formation of highly oxygenated organic molecules from aromatic compounds, Atmospheric Chem. Phys., 18, 1909–1921, 2018.

Pan, Y., Quan, J., Ma, P., Liao, Z., Jia, X., Dou, Y., Cheng, Z., Lei, L., Wang, Y., Zheng, M., Lü, D., and Wang, Y.: Mineral dust scavenges anthropogenic aerosols in polluted environment, Atmos. Environ., 309, 119938, 2023.

Peng, J., Hu, M., Shang, D., Wu, Z., Du, Z., Tan, T., Wang, Y., Zhang, F., and Zhang, R.: Explosive Secondary Aerosol Formation during Severe Haze in the North China Plain, Environ. Sci. Technol., 55, 2189–2207, 2021.

Qin, X., Chen, Z., Gong, Y., Dong, P., Cao, Z., Hu, J., and Xu, J.: Persistent Uptake of H2 O2 onto Ambient PM2.5 via Dark-Fenton Chemistry, Environ. Sci. Technol., 56, 9978–9987, 2022.

Rissanen, M.: Anthropogenic Volatile Organic Compound (AVOC) Autoxidation as a Source of Highly Oxygenated Organic Molecules (HOM), J. Phys. Chem. A, 125, 9027–9039, 2021.

Shi, X., Huang, G., Yang, D., Zhang, Q., Zong, W., Cheng, J., Sui, X., Yuan, F., and Wang, W.: Theoretical study of the formation and nucleation mechanism of highly oxygenated multi-functional organic compounds produced by α-pinene, Sci. Total Environ., 780, 146422, 2021.

Suh, I., Zhang, R., Molina, L. T., and Molina, M. J.: Oxidation Mechanism of Aromatic Peroxy and Bicyclic Radicals from OH−Toluene Reactions, J. Am. Chem. Soc., 125, 12655–12665, 2003.

Sun, Y., Du, W., Fu, P., Wang, Q., Li, J., Ge, X., Zhang, Q., Zhu, C., Ren, L., Xu, W., Zhao, J., Han, T., Worsnop, D. R., and Wang, Z.: Primary and secondary aerosols in Beijing in winter: sources, variations andprocesses, Atmospheric Chem. Phys., 16, 8309–8329, 2016.

Tan, H., Cai, M., Fan, Q., Liu, L., Li, F., Chan, P. W., Deng, X., and Wu, D.: An analysis of aerosol liquid

478 water content and related impact factors in Pearl River Delta, Sci. Total Environ., 579, 1822–1830,
479 2017.
480 Wang, J., Chen, S., Qiu, X., Niu, W., Li, O., Zhu, C., Zhang, X., Yang, X., and Zhang, G.: Pollution
481 Characteristics of Atmospheric Carbonyl Compounds in a Large City of Northern China, J. Chem.,
482 2022, 1–13, 2022.
483 Wang, S., Newland, M. J., Deng, W., Rickard, A. R., Hamilton, J. F., Muñoz, A., Ródenas, M., Vázquez,
484 M. M., Wang, L., and Wang, X.: Aromatic Photo-oxidation, A New Source of Atmospheric Acidity,
485 Env. Sci Technol, 2020a.
486 Wang, T., Liu, Y., Deng, Y., Cheng, H., Yang, Y., Feng, Y., Zhang, L., Fu, H., and Chen, J.: Photochemical
487 Oxidation of Water-Soluble Organic Carbon (WSOC) on Mineral Dust and Enhanced Organic
488 Ammonium Formation, Environ. Sci. Technol., 54, 15631–15642, 2020b.
489 Watne, Å. K., Westerlund, J., Hallquist, Å. M., Brune, W. H., and Hallquist, M.: Ozone and OH-induced
490 oxidation of monoterpenes: Changes in the thermal properties of secondary organic aerosol (SOA),
491 J. Aerosol Sci., 114, 31–41, 2017.
492 Wu, X., Kong, Q., Lan, Y., Sng, J., and Yu, L. E.: Refined Sea Salt Markers for Coastal Cities Facilitating
493 Quantification of Aerosol Aging and PM2.5 Apportionment, Environ. Sci. Technol., 2024.
494 Xu, B., Zhang, G., Gustafsson, Ö., Kawamura, K., Li, J., Andersson, A., Bikkina, S., Kunwar, B., Pokhrel,
495 A., Zhong, G., Zhao, S., Li, J., Huang, C., Cheng, Z., Zhu, S., Peng, P., and Sheng, G.: Large
496 contribution of fossil-derived components to aqueous secondary organic aerosols in China, Nat.
497 Commun., 13, 5115, 2022.
498 Xu, L., Guo, H., Boyd, C. M., Klein, M., Bougiatioti, A., Cerully, K. M., Hite, J. R., Isaacman-VanWertz,
499 G., Kreisberg, N. M., Knote, C., Olson, K., Koss, A., Goldstein, A. H., Hering, S. V., De Gouw, J.,

Baumann, K., Lee, S.-H., Nenes, A., Weber, R. J., and Ng, N. L.: Effects of anthropogenic emissions on aerosol formation from isoprene and monoterpenes in the southeastern United States, Proc. Natl. Acad. Sci., 112, 37–42, 2015.

Xu, M., Hu, B., Zhao, S., Yan, G., Wen, T., and Zhao, X.: Size-resolved water-soluble organic carbon and its significant contribution to aerosol liquid water, Sci. Total Environ., 927, 172396, 2024.

Xu, W., Han, T., Du, W., Wang, Q., Chen, C., Zhao, J., Zhang, Y., Li, J., Fu, P., Wang, Z., Worsnop, D. R., and Sun, Y.: Effects of Aqueous-Phase and Photochemical Processing on Secondary Organic Aerosol Formation and Evolution in Beijing, China, Environ. Sci. Technol., 51, 762–770, 2017.

Yang, W., Ma, J., Yang, H., Li, F., and Han, C.: Photoenhanced sulfate formation by the heterogeneous uptake of SO2 on non-photoactive mineral dust, Atmospheric Chem. Phys., 24, 6757–6768, 2024.

Yao, D., Guo, H., Lyu, X., Lu, H., and Huo, Y.: Secondary organic aerosol formation at an urban background site on the coastline of South China: Precursors and aging processes, Environ. Pollut., 309, 119778, 2022.

Ye, C., Chen, H., Hoffmann, E. H., Mettke, P., Tilgner, A., He, L., Mutzel, A., Brüggemann, M., Poulain, L., Schaefer, T., Heinold, B., Ma, Z., Liu, P., Xue, C., Zhao, X., Zhang, C., Zhang, F., Sun, H., Li, Q., Wang, L., Yang, X., Wang, J., Liu, C., Xing, C., Mu, Y., Chen, J., and Herrmann, H.: Particle-Phase Photoreactions of HULIS and TMIs Establish a Strong Source of H2 O2 and Particulate Sulfate in the Winter North China Plain, Environ. Sci. Technol., 55, 7818–7830, 2021.

Yu, G.-H., Park, S., and Lee, K.-H.: Source contributions and potential source regions of size-resolved water-soluble organic carbon measured at an urban site over one year, Environ. Sci. Process. Impacts, 18, 1343–1358, 2016.

Yu, Z. and Jang, M.: Atmospheric Processes of Aromatic Hydrocarbons in the Presence of Mineral Dust

Particles in an Urban Environment, ACS Earth Space Chem., 2019.

Zhan, B., Zhong, H., Chen, H., Chen, Y., Li, X., Wang, L., Wang, X., Mu, Y., Huang, R.-J., George, C., and Chen, J.: The roles of aqueous-phase chemistry and photochemical oxidation in oxygenated organic aerosols formation, Atmos. Environ., 266, 118738, 2021.

Zhang, X., Lambe, A. T., Upshur, M. A., Brooks, W. A., Gray Bé, A., Thomson, R. J., Geiger, F. M., Surratt, J. D., Zhang, Z., Gold, A., Graf, S., Cubison, M. J., Groessl, M., Jayne, J. T., Worsnop, D. R., and Canagaratna, M. R.: Highly Oxygenated Multifunctional Compounds in α-Pinene Secondary Organic Aerosol, Environ. Sci. Technol., 51, 5932–5940, 2017a.

Zhang, X., Li, J., Mo, Y., Shen, C., Ding, P., Wang, N., Zhu, S., Cheng, Z., He, J., Tian, Y., Gao, S., Zhou, Q., Tian, C., Chen, Y., and Zhang, G.: Isolation and radiocarbon analysis of elemental carbon in atmospheric aerosols using hydropyrolysis, Atmos. Environ., 198, 381–386, 2019.

Zhang, Y., Cai, J., Wang, S., He, K., and Zheng, M.: Review of receptor-based source apportionment research of fine particulate matter and its challenges in China, Sci. Total Environ., 586, 917–929, 2017b.